

Human guanylate-binding protein 1 as a model system investigated by several surface techniques

Andreas Kerstan

Department of Physical Chemistry I, University of Bochum, 44801 Bochum, Germany

Tatjana Ladnorg

Institute of Functional Interfaces, Karlsruhe Institute of Technology, 76344 Karlsruhe, Germany

Christian Grunwald

Institute of Biochemistry, Biocenter N210, J. Wolfgang Goethe-University, 60438 Frankfurt, Germany

Tobias Vöpel

Department of Physical Chemistry I, University of Bochum, 44801 Bochum, Germany

Denise Zacher

Department of Anorganic Chemistry II, University of Bochum, 44801 Bochum, Germany

Christian Herrmann

Department of Physical Chemistry I, University of Bochum, 44801 Bochum, Germany

Christof Wöll^{a)}

Institute of Functional Interfaces, Karlsruhe Institute of Technology, 76344 Karlsruhe, Germany

(Received 8 September 2010; accepted 22 October 2010; published 14 December 2010)

In medical technologies concerning the surface immobilization of proteins in a defined orientation, maintaining their activity is a critical aspect. Therefore, in this study, the authors have investigated the activity of an elongated protein attached to a self-assembled monolayer supported streptavidin layer for different relative orientations of the protein with regard to the surface. Several mutants of this protein, human guanylate-binding protein 1 (hGBP1) showing GTPase catalytic activity, have been furnished with either one or two biotin anchors. Various independent methods that are based on different biophysical properties such as surface plasmon resonance, atomic force microscopy, and quartz crystal microbalance have been used to determine the orientation of the hGBP1 variants after anchoring them via a streptavidin-linker to a biotinylated surface. The activity of guanosine-triphosphate hydrolysis of hGBP1 monomers bound on the surface is found to depend on their orientation relative to the substrate, relating to their ability to form dimers with other neighboring anchored mutants; the maximum activity is lower than that observed in solutions, as might be expected from diffusion limitations at the solid/liquid interface on the one hand and prevention from homodimer formation due to immobilization on the other hand. © 2010 American Vacuum Society. [DOI: 10.1116/1.3516461]

I. INTRODUCTION

For many applications in medical and biotechnologies, the defined orientation of proteins on surfaces is an important issue. This applies to the development of biosensors where the active center of the protein should be oriented not to the surface but rather to the outer space. Also, the generation of protein microarrays designed as diagnostic tools or for pharmaceutical analysis relies on properly oriented proteins. Therefore, efforts have been pursued over the past years to develop methods allowing to control protein immobilization on a substrate in a defined and oriented manner.^{1–3} In the present study, we present a systematic study based on a variety of different biophysical techniques in order to characterize the orientation and enzymatic activity of the protein

human guanylate-binding protein 1 (hGBP1) anchored to a streptavidin covered surface via one or two biotin anchors attached to mutants of hGBP1.

hGBP1 is a protein with a molecular mass of 67 kDa and belongs to the superfamily of large GTPases.⁴ It is known to catalyze the hydrolysis of guanosine-triphosphate (GTP) and plays a crucial role in viral immune defense.^{5,6} Its expression is induced by interferons. All proteins of the large GTPases superfamily share a similar structure with a N-terminal GTPase domain (approximately 300 amino acids), a middle-domain (approximately 150–200 amino acids), and a GTPase-effector domain (100 amino acids), which is involved in catalysis and the oligomerization with other GTP-binding molecules.^{7,8} GTP-binding proteins bind GTP, guanosine-diphosphate, and guanosine-monophosphate with similar affinities⁹ and catalyze the hydrolysis of GTP in an enzyme concentration dependent manner.^{10–12} A hGBP1 homodimer is formed, leading to an increase in GTPase activity.

^{a)}Author to whom correspondence should be addressed; electronic mail: christof.woell@kit.edu

Streptavidin represents a homotetramer protein with a molecular mass of 53 kDa. Because of the tight binding of streptavidin to biotin and due to its two biotin binding pockets, each is placed on opposite faces of the molecule (yielding a total of four biotin binding pockets); this system has become a powerful tool to mediate attachment of biotinylated proteins to a surface. Multicomponent systems can be constructed in a layer by layer fashion onto a biotinylated surface^{13,14} by using streptavidin as a kind of linker between the surface and biotinylated proteins. Great advantages of the biotin-streptavidin system, which should be mentioned again at this point, are the high affinity and selectivity, which avoid most of the undesirable unspecific binding and increase the degree of reproducibility.¹⁵

It is important to note that with regard to the binding of biomolecules to surfaces, unspecific interactions of the involved biomolecules can rarely be excluded completely. The main problem of unspecific interactions is the undefined or imprecisely defined molecular arrangement of the participating biomolecules on the substrate.^{16–18} The emerging surface/protein complex is a result of a variety of different weak protein surface interactions,^{19,20} and usually precise structural information on the conformation of, e.g., an adsorbed protein does not exist. Therefore, we need a combination of direct [e.g., atomic force microscopy (AFM)] and indirect activity measurements to infer on the conformation and orientation of a protein on a surface. As a reference, proteophobic substrate, we have used self-assembled monolayers²¹ (SAMs) fabricated from polyethylene glycol (PEG)-thiols, a powerful approach to produce protein-resistant surfaces. Employing microcontact printing, the SAMs can also be laterally patterned, which allows for a precise and direct determination of the height of single or even a multicomponent architecture.^{22–34} Because of the great difference between length and width,³⁵ hGBP1 is a well suited system to reliably determine the orientation on the streptavidin covered surface from surface topographies as determined with AFM. Another reason for selecting hGBP1 as model system is its enzymatic activity: unspecifically bound proteins often unfold on the surface and lose their catalytic function.¹⁶ hGBP1 shows a GTP hydrolysis activity,^{11,12,36,37} so that by determining the hydrolysis rate, one can easily determine whether the protein is still native or has lost its tertiary structure.

In previous studies, we have investigated the mechanism of dimer formation of hGBP1 by mutational analysis and have determined various crystal structures of its large GTPase (LG) domain bound to different nucleotides. Unfortunately, so far, no structure of the full length protein in its dimerized state^{11,38–40} could be determined. It was suggested that hGBP1 forms homodimers after GTP binding in an elongated head to head orientation.³⁹ In this work, mutants of the protein with different biotin anchor positions were tested in order to yield surface-anchored hGBP1-proteins with different orientations. In the context of these investigations, AFM-based nanoshaving and grafting^{41,42} proved to be powerful methods to form two- or even three-dimensional patterns on

surfaces, which allows the differentiation of, for example, specific and nonspecific interactions, mono- and multilayers, or even molecules with different geometries and orientations. Together with microcontact printing,⁴³ two convenient and low-cost methods for investigating patterned surfaces exist, which offer the opportunity to perform high-quality differential height measurements on the same sample. The combination of AFM, surface plasmon resonance (SPR), and quartz crystal microbalance (QCM) allows the investigation of protein-protein interactions at physiological conditions with respect to orientation, kinetic aspects, and conformational changes.

SPR spectroscopy is the method of choice to determine the kinetics of protein-protein and protein-biomolecule interactions. The use of a QCM-D device is more suitable for determining the absolute thickness of the adsorbed protein layers by applying the viscoelastic Voigt model.⁴⁴

II. MATERIALS AND METHODS

A. Molecular biology, cloning, and expression of hGBP1 mutants

The so-called Cys-5 mutant of hGBP1 has the following point mutations: C12A, C270A, C311S, C396A, and C589S. These mutations were inserted by successive polymerase chain reaction reactions according to the instructions of Quick Change site directed mutagenesis kit (Stratagene). The mutant Q577C has a point mutation at position 577, replacing a glutamine by a cysteine residue, and the double mutant Q577C/K485C has an additional cysteine at residue 485.

All hGBP1 mutants were expressed in *Escherichia coli* strain BL21 (DE3) using a pQE80L vector (Qiagen, Germany). Recombinant proteins were purified, modifying a previously described protocol,⁷ where we abstained from using the reducing agent dithioerythritol (DTE) in the gel filtration buffer. DTE contains two thiol groups that can harm preformed SAMs by competing for covalent binding to the gold surface. Protein concentrations were determined by UV-absorbance at 276 nm ($\epsilon=44\,800\text{ M}^{-1}\text{ cm}^{-1}$) in a buffer containing 20 mM potassium phosphate and 6M guanidinium hydrochloride at pH 6.5.⁴⁵

The hGBP1 mutants were biotinylated according to the instructions of the Maleimide-PEG₁₁-Biotin biotinylation kit (Pierce, Rockford, IL). The reaction mixture was incubated on ice overnight for at least 12 h. For each reaction, a volume of 350 μl was used with protein concentrations at 200 μM . Biotinylation efficiency was determined by the (2-(4'-hydroxyazobenzene) benzoic acid (HABA) biotin quantitation kit (Pierce, Rockford, IL). For the unmodified Cys-5 mutant, no anchor could be identified. The single mutant Q577C and double mutant Q577C/K485C showed a molar labeling ratio of 1:1 and 1:2, respectively.

B. Substrate preparation for AFM, SPR, QCM, and activity measurements

For substrate preparation and surface functionalization, we followed a previously described route.¹³ Briefly, Au sub-

strates for the AFM measurements were prepared by depositing an 80 Å layer of titanium and, subsequently, 1200 Å of gold onto polished [100] silicon wafers (Prolog Semicore, Ltd.) using a Leybold Univac evaporator. Metal deposition was done at room temperature at a base pressure of about 10^{-7} bar. For SPR measurement, the same procedure was used but 12 Å of titanium and, subsequently, 485 Å of gold were deposited onto D263 thin glass (Schott).¹⁴ In the case of QCM measurements, 1000 Å of gold was deposited onto a quartz crystal sensor (14 mm diameter, highly polished 5 MHz crystal, QSX 301). After gold deposition, the mean square roughness of the gold layer was checked via AFM and was found to be less than 3 nm. For measurements of hGBP1 activity, polished silicon wafers with a [100] surface were coated with gold as described above for the AFM measurements (80 Å titanium and 1200 Å gold).

C. SAM formation and laterally structured SAMs

Clean, freshly prepared gold substrates were dipped into pure or mixed thiol solutions to prepare SAMs with the desired properties (e.g., with a fixed and well-defined biotin surface concentration).^{13,14} In this study, oligoethylene (OEG)- (Prochimnia, Cat. No. TH005-02; see Ref. 46 for the structure), OH- (Aldrich, product No. 674249; see Ref. 46 for the structure), and biotin-terminated (obtained from A. Terfort; see Ref. 46 for the structure) thiols were diluted into ultrapure ethanol (to a final concentration of 1 mM). Biotinylated SAMs were found to form well from OH- and biotin-thiol mixtures with OH-/biotin-ratios of 5:1 to 10:1.¹³ Typical incubation times ranged from several hours to overnight. The self-assembly of the thiols was checked by x-ray photoelectron spectroscopy and IR-spectroscopy (data not shown).

Laterally patterned SAMs can be prepared via microcontact printing.¹³ Here, we used polydimethylsiloxane stamps with a periodic pattern of $3 \times 3 \mu\text{m}^2$. First, the protein repellent OEG-thiol was printed onto the clean gold surface before the remaining unmodified gold areas were backfilled with a mixture of biotin- (10 mol %) and OH-terminated (90 mol %) thiols in ultrapure ethanol (total thiol concentration is 1 mM).

D. Protein-protein interactions probed by SPR

Multicomponent protein systems were investigated by SPR in order to get information about kinetic aspects, the total amount of adsorbed protein mass, and the stoichiometry of the investigated interactions. A dual channel surface plasmon resonance system (Reichert, SR7000DC) was used for the multiprotein component analysis. The adsorption of streptavidin ($c=0.4 \mu\text{M}$ –0.02 mg/ml, Invitrogen) was monitored, directly followed by the adsorption of a biotinylated hGBP1 mutant (1 μM). Streptavidin solution was always freshly diluted. Each biotinylated hGBP1 mutant was adsorbed to a freshly preadsorbed streptavidin layer. All measurements were carried out at a flow rate of 5 $\mu\text{l}/\text{min}$ and using buffer A (50 mM Tris, 5 mM MgCl_2 , $p\text{H}=7.9$). First, the SAM surface was rinsed for 5 min with buffer A,

then, streptavidin and the hGBP1 mutant were injected successively for defined time periods. Finally, the protein layers were rinsed for 20 min with buffer A to remove weakly adsorbed proteins.

E. Protein-protein interactions probed by quartz crystal microbalance

QCM measurements were performed in a QCM-D spectrometer (Q-sense E4 Auto). The QCM-substrates were mounted in a fluid cell with one side exposed to the buffer A solution. A flow rate of 15 $\mu\text{l}/\text{min}$ was chosen to efficiently exchange buffer and protein solutions. Under the chosen experimental conditions, a frequency shift of ± 1 Hz was detectable.

The gold surface of the quartz crystal substrates was covered with a mixed SAM grown from thiol solutions containing 10 mol % biotin-thiol and 90 mol % mercaptoundecan-1-ol. Then streptavidin (0.4 μM) was preadsorbed to the biotinylated SAM for 20 min before a single or double biotinylated hGBP1 mutant (1 μM) was allowed to interact with the surface immobilized streptavidin. The monitored runs were analyzed with the Q-SENSE software in consideration of the frequency and dissipation response. A viscoelastic model developed by Voigt⁴⁴ was used for the data analysis, which allowed the estimation of the thickness of the surface-bound protein layers.

F. hGBP1 mutant catalytic activity in solution and on a biofunctionalized gold surface

Activity measurements of the hGBP1 mutants were carried out as described before.^{36,37,47} First, the activity was measured in solution for both mutants at room temperature (20 °C). The concentrations were 0.5 μM for the protein and 50 μM for GTP. After defined incubation times, aliquots were analyzed by reversed phase chromatography using a Chromolith Performance RP-18 end capped column (Merck). The same procedure of analysis was applied to measure the hGBP1 activity on biofunctionalized surfaces. Gold coated, polished [100] silicon wafers served as substrate to grow mixed biotinylated SAMs (see substrate preparation above). Subsequently, the biotinylated SAM was incubated for 15 min with streptavidin (0.4 μM), and after extensive rinsing, one of the hGBP1 mutants (1 μM) was also incubated for 15 min with the streptavidin coated surface. After buffer rinsing, the surface was covered with a defined volume of 50 μM GTP in buffer A (50 μM ; 3 ml). GTP hydrolysis was analyzed by high pressure (performance) liquid chromatography with aliquots that were taken from the reaction mixture after different incubation times.

G. AFM measurement

1. Imaging conditions

AFM measurements were performed in the liquid cell of a MultiMode NanoScope IIIa AFM (Digital Instruments) fitted with a commercial Si_3N_4 cantilever of a normal spring constant of 0.12 N/m in buffer A. The microscope was operated

in tapping mode, where the tip was scanned back and forth at 90° along the horizontal line in a scan range of 15 μm . Image recordings were done with a 5 μm z -range and 150 μm x - and y -range scanner (type J Digital Instruments) without removing the liquid cell from the surface before and after the scanning process.

2. Nanoshaving

In performing nanoshaving, the microscope was operated in a constant force mode. A flat area was chosen on the substrate, so that a layer of defined thickness was shaved at all positions. Therefore, the cantilever runs with high and constant force twice over the determined area, to remove the SAM and protein multilayer from the surface, so that a rectangular hole remains. After the shaving, the cantilever was engaged to the surface to get a topographic picture.

III. RESULTS

A. SPR measurements

Controlling the amount of streptavidin adsorption to SAM surfaces by adjusting the biotin thiol concentration and studies about the real-time adsorption kinetics of streptavidin were reported previously.¹⁴ Here, we have employed the same procedures. In order to get a reproducible streptavidin layer, the basic parameters such as concentrations and incubation times for growing the biotinylated SAM as well as for adsorbing the streptavidin (0.4 μM) were kept constant. Thus, the results obtained for the different biotinylated hGBP1 mutants anchored to the preimmobilized streptavidin can be compared directly.

hGBP1 belongs to the dynamin superfamily of large GT-Pases and has a pronounced elongated shape, which can be directly derived from the crystal structure. This structure also reveals that 5 out of 9 cysteine residues present in the sequence of hGBP1 are exposed to the surrounding solvent and therefore are accessible to maleimide labeling.⁴⁸ In order to attach the biotin anchor specifically only to the desired positions 485 and 577, we used the Cys-5 mutant of hGBP1, where these five cysteine residues were replaced by serines and alanines in a first step. In a second step, cysteines were inserted at the designated positions 485 and 577 by mutagenesis.⁴⁸ This process yields the mutants Q577C (only one additional cysteine at position 577) and Q577C/K485C (two additional cysteines at positions 577 and 485). Position 577 is located in the small helix α 13 near the LG domain. The double-mutant Q577C/K485C carries an additional reactive cysteine at position 485 at the opposite side of hGBP1; thus, both ends of the elongated protein contain a biotin anchor (Fig. 1). In the following, these two mutants will be referred to as single mutant and double mutant, respectively. Considering these structural differences, one expects significant differences of the two hGBP1 variants with respect to their orientation on the surface.

In the first set of experiments, we monitored the adsorption of hGBP1 by SPR. Figure 2 shows the docking of streptavidin to the SAM consisting of 10% biotin thiol and

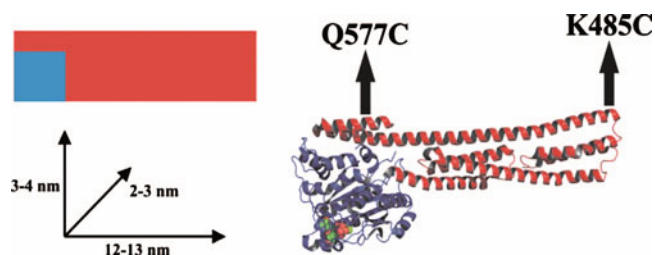


FIG. 1. (Color) Crystal structure of hGBP1 (PDB: 1dg 3) in ribbon presentation with the LG domain colored in blue and the helical domain in red. The two possible anchor positions; Cys485 and Cys577 are indicated. The rough dimensions of the protein are shown as well as a schematic representation of the protein as it is used in Fig. 7; note the same color code as in the ribbon presentation.

90% mercaptoundecan-1-ol, followed by the binding of the two biotinylated hGBP1 mutants. The loading with streptavidin toward biotinylated SAMs allows precise control of immobilization density as shown by the equal streptavidin adsorption steps for both measurements.

From the SPR data, the amount of adsorbed streptavidin (1500 RU) was found to amount to 145 ng/cm^2 . The same result was obtained in both measurements; this value corresponds to a density of 41% streptavidin on the surface (footprint: $23 \times 85 \text{ nm}^2$).⁴⁹ The deviation in the amount of streptavidin adsorption was less than 10%, which underlines the high reproducibility of streptavidin binding to biotin. As expected, washing with buffer does not cause any dissociation. Subsequent adsorption of the single biotinylated Q577C mutant and the double biotinylated Q577C/K485C mutant, respectively, shows fast kinetics, which indicates highly specific binding of biotinylated hGBP1 to the immobilized streptavidin. Additionally, one can clearly recognize the saturation of the adsorption for both mutants. Importantly, the total adsorption of the single mutant Q577C is about three times higher (approximately 215 ng/cm^2) than for the double hGBP1 mutant (77 ng/cm^2). In the case of the single biotinylated mutant, the adsorbed mass suggests an approximately 1:1 molar ratio of hGBP1 to streptavidin, while for the double biotinylated mutant, a 1:3 ratio is found.

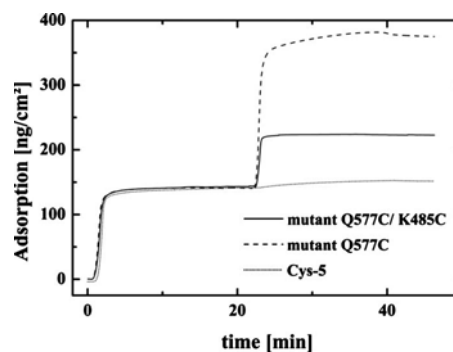


FIG. 2. Subsequent adsorption of streptavidin and hGBP1. Solid line: double biotinylated hGBP1 (Q577C/K485C), dashed line: single biotinylated hGBP1 (Q577C), and dotted line: Cys-5 without biotinylation as a control. For SAM formation, the content of biotin thiol was kept constant at 10%.

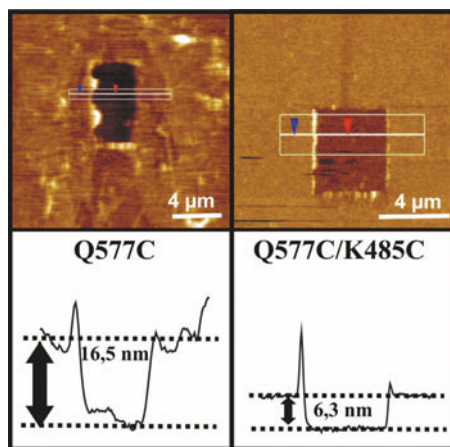


FIG. 3. (Color) Topographic height image after adsorption of hGBP1 mutants (left: Q577C; right: Q577C/K485C) after streptavidin incubation on a biotin-SAM. The rectangular hole in the middle was caused by scraping the surface with the cantilever and thereby moving the SAM and the proteins aside. The height contrast is shown in the lower panels.

B. AFM

Atomic force microscopy can not only be used for imaging the topography but is also a versatile tool for manipulation and structuring of biological surfaces. The applied loading force is the main parameter to switch between imaging and manipulation. During imaging, the loading forces are minimized to prevent any deformation of the biological structures under investigation. Upon increasing the load in localized predefined areas, adsorbed molecules can be removed in a straightforward fashion. This methodology is known as nanoshaving.^{41,42} In Fig. 3, the AFM micrographs recorded for a patterned SAM after incubation with streptavidin and hGBP1 in tapping mode are presented. The tapping mode reduced forces exerted on the sample to a minimum and was used to avoid compression of the protein layers. The square hole visible in the middle of the image was created by nanoshaving. Note that some of the removed protein material accumulate at the left and right borders of the nanoshaved square. In the cross section, these accumulated protein remnants result in pronounced spikes close to the protein-free area. The section analysis also reveals the absence of compression of the protein multicomponent system during the measurements.

For both mutants, the images reveal the presence of a densely packed and homogeneous protein adlayer. By using the SCANNING PROBE IMAGE PROCESSOR software package (Image Metrology, Hørsholm), an average height profile (cross-section analysis) of a well-defined area (white rectangle in the image) could be obtained. For the multicomponent layer of streptavidin plus hGBP1, mutant heights of 165 ± 10 Å for the single biotinylated and 63.4 ± 10 Å for the double biotinylated hGBP1 mutant were observed. The difference in the height of streptavidin 42.2 ± 10 Å, which is reported in previous studies¹⁰ and which equals the dimension obtained from the crystal structure of streptavidin, amounts to 122.8 ± 10 Å for the single mutant (Q577C) and

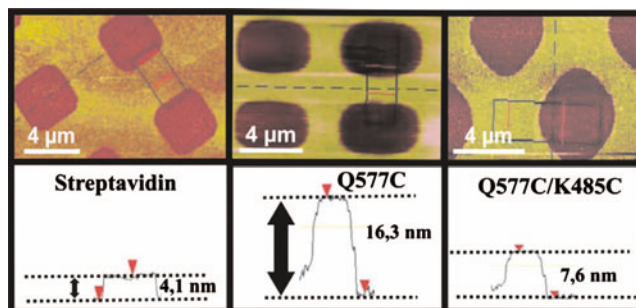


FIG. 4. (Color) Topographic height images after incubation with streptavidin (left) and after additional incubation with the single biotinylated hGBP1 (Q577C) (middle) and the double biotinylated hGBP1 (Q577C/K485C) (right), respectively. The dark regions indicate the stamp areas (microprinting) where protein-resistant OEG (6) thiol was incubated, whereas the bright bridges show the regions preloaded with biotin-thiol (10 mol %), streptavidin, and/or hGBP1.

21.2 ± 10 Å for the double mutant (Q577C/K485C). In order to exclude that in the shaving process, the SAM and protein layers were only partially removed; some control experiments were carried out with the SAMs' lateral structure via microcontact printing. The biotinylated regions (stripes) of the sample can be recognized as bright stripes in contrast to the dark 3×3 μm^2 squares (Fig. 4). The measured heights are in good agreement with the results obtained by mechanical scraping of patterns via nanoshaving. The differences are clearly within the experimental error bars.

Comparing the results obtained for the heights of the protein adlayers with the dimensions of hGBP1 taken from its crystal structure (Fig. 1), the obtained values for single and double biotinylated hGBP1 match well with the length (120–130 Å) of hGBP1 and its width (30–40 Å), respectively. Furthermore, taking the dimensions of the elongated hGBP1 molecule in consideration, a 3–4 times larger footprint is calculated for this protein when lying alongside on a surface (39 nm^2) as compared to an upright orientation (12 nm^2). The SPR measurements revealed a three times higher adsorption for the single biotinylated variant of hGBP1 in comparison to the double biotinylated species. This observation is fully consistent with the hGBP1 mutant bound with two anchors on opposite sides, resulting in a lying orientation (long axis parallel to substrate) while the single biotinylated mutant is adsorbed in an upright orientation.

C. QCM

In contrast to SPR, the QCM-D technique does not only allow determining the mass of very thin surface-bound layers but also simultaneously yields information about their structural (viscoelastic) properties by measuring the protein-induced dissipation. By using measurements at multiple frequencies and additionally detecting dissipation, this method offers the opportunity to determine the thickness as well as the viscosity and elasticity by employing a viscoelastic mathematic model.

For reasons of verification and substantiation, the thicknesses of the streptavidin and hGBP1 layers were measured

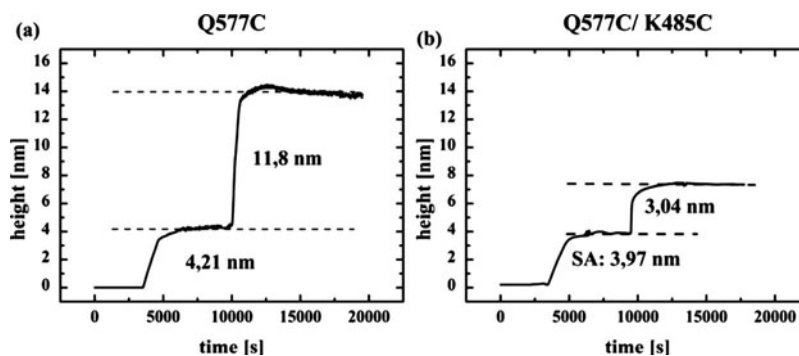


FIG. 5. QCM-D measurements documenting streptavidin binding and subsequent incubation with hGBP1 (single biotinylated on the left and double biotinylated on the right). By measuring at multiple frequencies and applying a viscoelastic model (Voigt model) incorporated in Q-SENSE software Q-tools, the thickness of the adhering film (streptavidin+hGBP1 mutant) was calculated.

by QCM-D and compared to the heights obtained by AFM. Figure 5 shows the step heights of both mutants Q577C and Q577C/K485C.

The used multiple frequency data are shown in Ref. 46 (Fig. 2). The height of the streptavidin adlayer is found to amount to 40 ± 10 Å in both cases. This value compares well with the size of streptavidin in its crystal structure. For the calculated thicknesses of the two hGBP1 mutants, we find a perfect agreement of the SPR and AFM results. The difference from the height of streptavidin amounts to 118 ± 10 Å for the single mutant and 30.4 ± 10 Å for the double mutant. The postulated assumption that the two hGBP1 mutants show a rather different behavior concerning docking and orientation on the streptavidin terminated surface is thus fully corroborated by the QCM-D data. Although the applied viscoelastic model is only an approximation, it allows clearly distinguishing between the two hGBP1 mutants. The QCM-D results provide a direct, solid, and independent confirmation for the different docking orientations of the hGBP1 mutants when binding to the preimmobilized layer of streptavidin.

D. Activity test

hGBP1 shows a characteristic enzymatic activity: it catalyzes the hydrolysis of GTP. This biochemical property is exploited to find out if hGBP1 maintains its catalytic activity after biotinylation and after anchoring it to the streptavidin grafted to the substrate. In a $50 \mu\text{M}$ GTP solution at 25°C , the catalytic turnover numbers amount to 17.0 and 14 min^{-1} for the single biotinylated mutant Q577C and double biotinylated mutant Q577C/K485C, respectively. These values are in good agreement with the value of 33.9 min^{-1} reported for the unmodified Cys-5 mutant⁴² taking into account the K_M effect of higher GTP concentration ($350 \mu\text{M}$ in that study instead of $50 \mu\text{M}$).¹² In GTP concentration dependent activity studies, it could be shown that a sevenfold higher substrate concentration leads to approximately two to threefold higher activity. For technical reasons, the selected substrate concentration had to be lower in this study than in

common practice. At $350 \mu\text{M}$, the relative change of GTP concentration would be too small in experiments with surface-bound hGBP1 to be detected.

These results clearly demonstrate that the protein retains enzymatic activity after biotinylation. For the following, it has to be noted that in the presence of GTP, the hGBP1 will form dimers, which show a substantially higher activity than hGBP1 monomers.^{10,37,39} By analyzing the results obtained for a highly diluted hGBP1 in solution (where the fraction of monomers exceeds that of dimers), a value of about $2\text{--}3 \text{ min}^{-1}$ is obtained for the activity of a single hGBP1 monomer.¹¹

Intriguingly, after anchoring to the substrate for both mutants, the obtained activities are significantly reduced. The single mutant Q577C shows an activity of 3 min^{-1} on the surface, 4.5 times lower than in solution. For the double mutant Q577C/K485C, the hydrolytic activity on the surface amounts to 7 min^{-1} (Fig. 6), 2–4 times lower than in solution. For a comparison of the surface activities with those measured in solution, we first have to discuss whether the surface-bound hGBP1 can be dimerized. In fact, from a comparison to the x-ray structure of the LG domain dimer,³⁹ we conclude that the single biotinylated hGBP1 protein oriented upright and head (LG domain) down on the surface as suggested in Fig. 7 cannot form a head to head dimer. Accordingly, the Q577C mutant can only be present in the form of a monomer; the activity of 3 min^{-1} thus compares well with the monomer activity found in a highly diluted protein solution ($2\text{--}3 \text{ min}^{-1}$). One would expect the activity of the surface-bound monomer to be smaller than that of monomers in solution because of the limited diffusion of GTP in the vicinity of the surface.¹⁴

The surface-anchored double biotinylated hGBP1 shows an activity higher than that measured for the monomer activity in solution. The protein is oriented alongside on the surface, which in principle could allow for dimer formation in the required head to head orientation of two neighboring protein molecules (see Fig. 7). We speculate that a fraction of the immobilized proteins are able to move within the limits of their anchoring such that head-to-head dimers are formed. A fraction of hGBP1 present in the form of dimers would

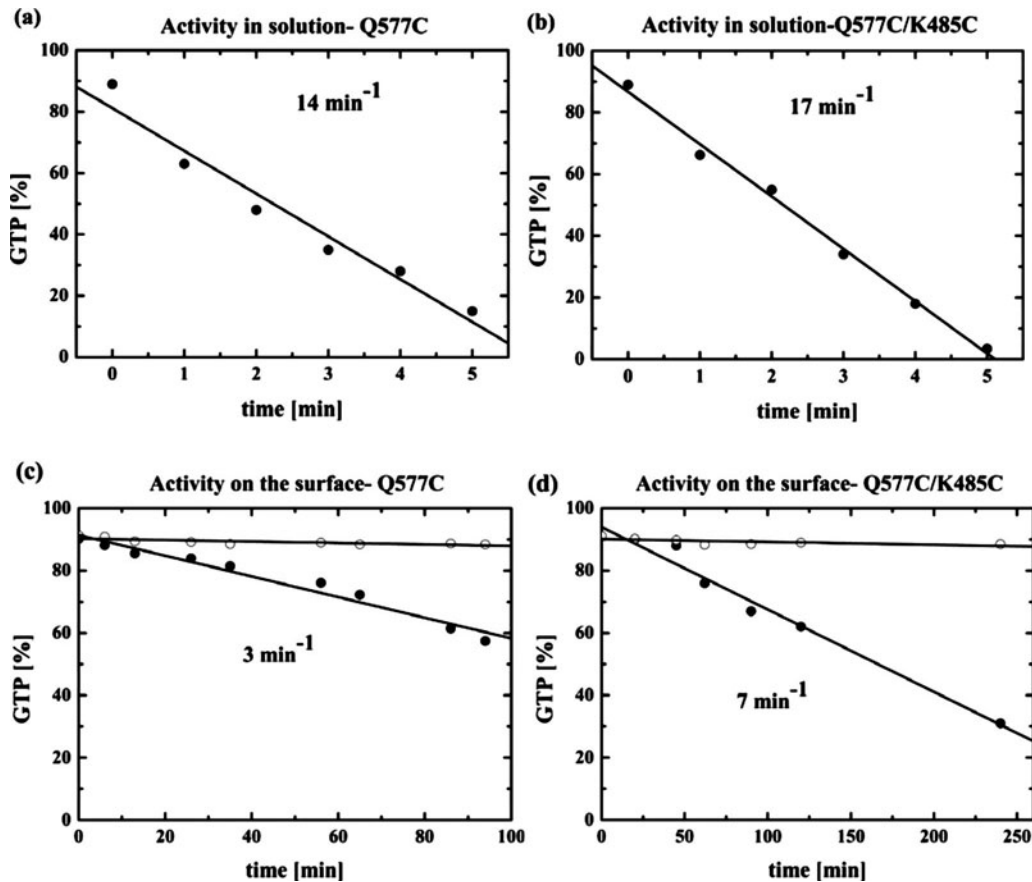


FIG. 6. Specific GTPase activity of hGBP1 in solution (upper panels) and on the surface (lower panels). The measurements in solution were performed at concentrations of $0.5 \mu\text{M}$ hGBP1 and $50 \mu\text{M}$ GTP. For the calculation of specific activity on the surface, the amount of immobilized hGBP1 was derived from the SPR measurements. The volume of buffer ($V=2.5 \text{ ml}$) coating the gold surface and the surface area (78.5 cm^2) were taken into account for the calculation of the enzyme quantity and the resulting specific activity indicated in the figure. Gold wafers without hGBP1 coating were used as a reference (open circles).

explain the rather high GTP hydrolysis activity observed in this case. On the basis of the present data, however, we feel unable to answer this question conclusively; additional data will be required to resolve this issue.

IV. CONCLUSIONS

We have investigated the attachment of the elongated protein hGBP1 on a solid surface. Anchoring was achieved by fabricating two mutants of hGBP1 with one and two biotin anchors which bind to a streptavidin adlayer. By employing a number of different independent techniques such as SPR, AFM, and QCM, a detailed and consistent picture of the hGBP1 adlayer is obtained. For the doubly anchored mutant, we propose an alongside orientation with the long axis of the hGBP1 orientated parallel to the surface plane, whereas for the single-anchor mutant, a near-upright orientation is found. The GTP hydrolysis catalytic activity, although lower than in solution, indicates full integrity for both of the surface-bound protein mutants. These studies render a starting point for further investigations of hGBP1 and other enzymes with regard to a correlation between their orientation and activity. In particular, attachment of a protein in a restricted manner allows addressing the importance of structural constraints

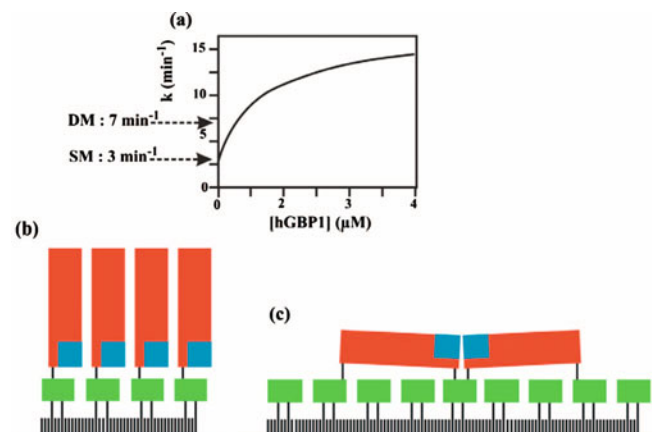


FIG. 7. (Color) (a) Schematic presentation of the concentration dependent GTPase activity of hGBP1 in solution in the presence of $50 \mu\text{M}$ GTP (calculated from Refs. 9 and 35); the activities observed here for surface-bound single mutant and double mutant of hGBP1 are indicated by arrows. Suggested orientations of hGBP1 (b) single mutant and (c) double mutant are shown schematically using the representation of the hGBP1 molecule in Fig. 1 (streptavidin in green).

when interactions with partner proteins come into play, e.g., in a homodimer complex. The methods presented in this study can be employed for investigations of the structural and kinetic properties of protein complexes attached in a defined orientation on a surface.

- ¹C. Grunwald, K. Schulze, A. Reichel, V. U. Weiss, D. Blaas, J. Piehler, K.-H. Wiesmüller, and R. Tampé, *Proc. Natl. Acad. Sci. U.S.A.* **107**, 6146 (2010).
- ²L. S. Wong, F. Khan, and J. Micklefield, *Chem. Rev. (Washington, D.C.)* **109**, 4025 (2009).
- ³S. Lata, A. Reichel, R. Brock, R. Tampé, and J. Piehler, *J. Am. Chem. Soc.* **127**, 10205 (2005).
- ⁴H. R. Bourne, D. A. Sanders, and F. McCormick, *Nature (London)* **348**, 125 (1990).
- ⁵S. L. Anderson, J. M. Carton, J. Lou, L. Xing, and B. Y. Rubin, *Virology* **256**, 8 (1999).
- ⁶P. Staeheli, F. Pitossi, and J. Pavlovic, *Trends Cell Biol.* **3**, 268 (1993).
- ⁷G. J. K. Praefcke, M. Geyer, M. Schwemmler, H. R. Kalbitzer, and C. Herrmann, *J. Mol. Biol.* **292**, 321 (1999).
- ⁸S. Sever, H. Damke, and S. L. Schmid, *J. Cell Biol.* **150**, 1137 (2000).
- ⁹Y. S. Cheng, C. E. Patterson, and P. Staeheli, *Mol. Cell. Biol.* **11**, 4717 (1991).
- ¹⁰B. Prakash, L. Renault, G. J. K. Praefcke, C. Herrmann, and A. Wittinghofer, *EMBO J.* **19**, 4555 (2000).
- ¹¹S. Kunzelmann, G. J. Praefcke, and C. Herrmann, *J. Biol. Chem.* **281**, 28627 (2006).
- ¹²M. Schwemmler and P. Staeheli, *J. Biol. Chem.* **269**, 11299 (1994).
- ¹³C. Grunwald, W. Eck, N. Opitz, J. Kuhlmann, and C. Wöll, *Phys. Chem. Chem. Phys.* **6**, 4358 (2004).
- ¹⁴R. Chelmoski, A. Prekelt, C. Grunwald, and C. Wöll, *J. Phys. Chem. A* **111**, 12295 (2007).
- ¹⁵H.-L. Schmidt, W. Schumann, and F. Scheller, *Specific Features of Biosensors Sensors, A Comprehensive Survey* (Verlag Chemie, Weinheim, 1992), Vol. 1, pp. 719–801.
- ¹⁶C. Czeslik, *Z. Phys. Chem.* **218**, 771 (2004).
- ¹⁷C. Czeslik, G. Jackler, and C. Royer, *Spectroscopy* **16**, 139 (2002).
- ¹⁸W. Norde, *Macromol. Symp.* **103**, 5 (1996).
- ¹⁹V. Ball, A. Bentaleb, J. Hemmerle, J.-C. Voegel, and P. Schaaf, *Langmuir* **12**, (1996).
- ²⁰C. Calonder, Y. Tie, and P. R. van Tassel, *Proc. Natl. Acad. Sci. U.S.A.* **98**, 10664 (2001).
- ²¹M. Kind and C. Wöll, *Prog. Surf. Sci.* **84**, 230 (2009).
- ²²E. Ostuni, R. G. Chapman, M. N. Liang, G. Meluleni, G. Pier, D. E. Ingber, and G. M. Whitesides, *Langmuir* **17**, 6336 (2001).
- ²³K. L. Prime and G. M. Whitesides, *J. Am. Chem. Soc.* **115**, 10714 (1993).
- ²⁴S. Herrwerth, T. Rosendahl, C. Feng, J. Fick, W. Eck, M. Himmelhaus, R. Dahint, and M. Grunze, *Langmuir* **19**, 1880 (2003).
- ²⁵R. G. Chapman, E. Ostuni, S. Takayama, R. E. Holmlin, L. Yan, and G. M. Whitesides, *J. Am. Chem. Soc.* **122**, 8303 (2000).
- ²⁶R. G. Chapman, E. Ostuni, L. Yan, and G. M. Whitesides, *Langmuir* **16**, 6927 (2000).
- ²⁷S. Herrwerth, W. Eck, S. Reinhardt, and M. Grunze, *J. Am. Chem. Soc.* **125**, 9359 (2003).
- ²⁸A. J. Pertsin, M. Grunze, and I. A. Garbuzova, *J. Phys. Chem. B* **102**, 4918 (1998).
- ²⁹A. J. Pertsin and M. Grunze, *Langmuir* **16**, 8829 (2000).
- ³⁰A. J. Pertsin, T. Hayashi, and M. Grunze, *J. Phys. Chem. B* **106**, 12274 (2002).
- ³¹K. Prime and G. Whitesides, *Science* **252**, 1164 (1991).
- ³²B. P. Lee, J. L. Dalsin, and P. B. Messersmith, *Biomacromolecules* **3**, 1038 (2002).
- ³³*Poly(ethylene Glycol) Chemistry: Biotechnical and Biomedical Applications*, edited by J. M. Harris (Plenum, New York, 1992), Vol. 43, pp. 233–234.
- ³⁴E. Ostuni, R. G. Chapman, R. E. Holmlin, S. Takayama, and G. M. Whitesides, *Langmuir* **17**, 5605 (2001).
- ³⁵B. Prakash, G. J. K. Praefcke, L. Renault, A. Wittinghofer, and C. Herrmann, *Nature (London)* **403**, 567 (2000).
- ³⁶S. Kunzelmann, G. J. Praefcke, and C. Herrmann, *Methods Enzymol.* **404**, 512 (2005).
- ³⁷G. J. K. Praefcke, S. Kloep, U. Benschid, H. Lilie, B. Prakash, and C. Herrmann, *J. Mol. Biol.* **344**, 257 (2004).
- ³⁸G. J. K. Praefcke and H. T. McMahon, *Nat. Rev. Mol. Cell Biol.* **5**, 133 (2004).
- ³⁹A. Ghosh, G. J. K. Praefcke, L. Renault, A. Wittinghofer, and C. Herrmann, *Nature (London)* **440**, 101 (2006).
- ⁴⁰K. Scheffzek, M. R. Ahmadian, W. Kabsch, L. Wiesmüller, A. Lautwein, F. Schmitz, and A. Wittinghofer, *Science* **277**, 333 (1997).
- ⁴¹Y. Xia, J. A. Rogers, K. E. Paul, and G. M. Whitesides, *Chem. Rev. (Washington, D.C.)* **99**, 1823 (1999).
- ⁴²S. Xu and G. Liu, *Langmuir* **13**, 127 (1997).
- ⁴³D. Qin, Y. Xia, and G. M. Whitesides, *Nat. Protoc.* **5**, 491 (2010).
- ⁴⁴M. Meyers and K. Chawla, *Mechanical Behaviors of Materials*, 1st ed (Prentice-Hall, Upper Saddle River, NJ, 1999), Sec. 13.10, pp. 570–580.
- ⁴⁵S. C. Gill and P. H. von Hippel, *Anal. Biochem.* **182**, 319 (1989).
- ⁴⁶See supplementary material at E-BJIOBN-5-303004 for the chemical structure of the used thiols (Fig. 1) and the QCM multiple frequency and dissipation data (Fig. 2) used for the calculation of the thickness of the adsorbed protein films.
- ⁴⁷T. Vöpel, A. Syguda, N. Britzen-Laurent, S. Kunzelmann, M.-B. Lüdemann, C. Dovengerds, M. Stürzl, and C. Herrmann, *J. Mol. Biol.* **400**, 63 (2010).
- ⁴⁸T. Vöpel, S. Kunzelmann, and C. Herrmann, *FEBS Lett.* **583**, 1923 (2009).
- ⁴⁹E. Ostuni, L. Yan, and G. M. Whitesides, *Colloids Surf., B* **15**, 3 (1999).